# Distribution of $\alpha$ 2 -Adrenergic Receptors in the Living Human Brain Using [ 11 C]yohimbine PET

Chloé Laurencin, Sophie Lancelot, Inès Merida, Nicolas Costes, Jérôme Redouté, Didier Le Bars, Philippe Boulinguez, Bénédicte Ballanger

biomolecules

MDPI

*Article*

# Distribution of $\alpha_2$-Adrenergic Receptors in the Living Human Brain Using [$^{11}$C]yohimbine PET

**Chloé Laurencin [1,2,3,4,5], Sophie Lancelot [1,2,3,4,6,7], Inès Merida [6], Nicolas Costes [6], Jérôme Redouté [6], Didier Le Bars [6,7], Philippe Boulinguez [1,2,3,4] and Bénédicte Ballanger [1,2,3,4,*]**

1 Université de Lyon, 69622 Lyon, France; chloe.laurencin@chu-lyon.fr (C.L.); sophie.lancelot@univ-lyon1.fr (S.L.); philippe.boulinguez@univ-lyon1.fr (P.B.)
2 Université Claude Bernard Lyon 1, 69100 Villeurbanne, France
3 INSERM U1028, Lyon Neuroscience Research Center (CRNL), 69000 Lyon, France
4 CNRS UMR5292, Lyon Neuroscience Research Center (CRNL), 69000 Lyon, France
5 Hôpital Neurologique Pierre Wertheimer, Service de Neurologie C, Centre Expert Parkinson, Hospices Civils de Lyon, 69677 Bron, France
6 CERMEP-Imagerie du Vivant, 69500 Bron, France; ines.merida@cermep.fr (I.M.); costes@cermep.fr (N.C.); redoute@cermep.fr (J.R.)
7 Hospices Civils de Lyon, 69677 Bron, France
* Correspondence: benedicte.ballanger@cnrs.fr

**Abstract:** The neurofunctional basis of the noradrenergic (NA) system and its associated disorders is still very incomplete because in vivo imaging tools in humans have been missing up to now. Here, for the first time, we use [$^{11}$C]yohimbine in a large sample of subjects (46 healthy volunteers, 23 females, 23 males; aged 20–50) to perform direct quantification of regional alpha 2 adrenergic receptors' ($\alpha_2$-ARs) availability in the living human brain. The global map shows the highest [$^{11}$C]yohimbine binding in the hippocampus, the occipital lobe, the cingulate gyrus, and the frontal lobe. Moderate binding was found in the parietal lobe, thalamus, parahippocampus, insula, and temporal lobe. Low levels of binding were found in the basal ganglia, the amygdala, the cerebellum, and the raphe nucleus. Parcellation of the brain into anatomical subregions revealed important variations in [$^{11}$C]yohimbine binding within most structures. Strong heterogeneity was found in the occipital lobe, the frontal lobe, and the basal ganglia, with substantial gender effects. Mapping the distribution of $\alpha_2$-ARs in the living human brain may prove useful not only for understanding the role of the NA system in many brain functions, but also for understanding neurodegenerative diseases in which altered NA transmission with specific loss of $\alpha_2$-ARs is suspected.

**Keywords:** $\alpha_2$-adrenoceptor; [$^{11}$C]yohimbine; hybrid PET/MRI; human; cartography; in vivo



**Citation:** Laurencin, C.; Lancelot, S.; Merida, I.; Costes, N.; Redouté, J.; Le Bars, D.; Boulinguez, P.; Ballanger, B. Distribution of $\alpha_2$-Adrenergic Receptors in the Living Human Brain Using [$^{11}$C]yohimbine PET. *Biomolecules* **2023**, *13*, 843. https://doi.org/10.3390/biom13050843

Academic Editors: Anne M. Landau, Francisco R. Lopez-Picon and Nadja Van Camp

Received: 27 April 2023
Revised: 12 May 2023
Accepted: 12 May 2023
Published: 15 May 2023



## 1. Introduction

The noradrenergic (NA) system has been implicated in the regulation of brain regions involved in numerous motor and non-motor functions, in particular arousal, sensory processing, attention, working memory, cognitive control, reward, mood, and emotion [1–4]. Accordingly, disruptions of NA functions have been associated with several disorders, with a potentially important role in neurodegenerative diseases [5–10]. This makes the NA system an important molecular target for drug development [11–15]. However, knowledge of the neurofunctional basis of the NA system on which such an endeavor is based is still incomplete and highly controversial. A major reason for the lack of knowledge is the lack of specific in vivo imaging tools in humans.

Detailed mapping of anatomical distribution of $\alpha_2$-adrenergic receptors (ARs) in the human brain is essential for understanding the neurochemistry of neurodegenerative and neuropsychiatric disorders. Until now, it has only been studied ex vivo using quantitative autoradiography [16–24]. Although these studies have provided important insights, they have

substantial limitations inherent to the technique. Findings obtained with autoradiography have highlighted dramatic species differences in the levels of $\alpha_2$-ARs [18] in several brain areas, making it difficult to extrapolate findings from animals to humans and complicating the interpretation of behavioral studies in rodents. The results obtained with autoradiography in humans are based on fragmentary analyses, and caveats are found in the restrictions of the tissue samples analyzed, such as samples of the human frontal cortex only related to Brodmann's area 10 [22] or Brodmann's area 9 [17,25]. Finally, autoradiography findings are limited by the sample size that can be used (ranging from 2 [26] to 22 [21] subjects).

In vivo imaging of the NA system has recently become feasible in humans with the development of a novel PET radiotracer: the [$^{11}$C]yohimbine [27,28]. [$^{11}$C]yohimbine binds with high selectivity to all $\alpha_2$-ARs subtypes [29]. This represents a great opportunity to fill in missing data in the living human brain by directly quantifying regional $\alpha_2$-AR availability. Here, for the first time, we use [$^{11}$C]yohimbine in a large sample of subjects to map the distribution of $\alpha_2$-ARs in the living human brain.

## 2. Materials and Methods

### *2.1. Participants*

Forty-six healthy subjects (23 males (mean age ± SD, 35.1 ± 9.4; range 20–50 y) and 23 females (mean age ± SD, 35.5 ± 9; range 20–50 y)) were selected to participate in the study. Male and female subjects were recruited to achieve a homogeneous age distribution between 20 and 50 years old. Exclusion criteria were as follows: ferromagnetic implanted materials, claustrophobia, pregnancy, history of noradrenergic medications, history of dependence on alcohol or other drugs of abuse, diagnosis of other neurological or psychiatric disorders, and history of head trauma. None of the participants were smokers.

### *2.2. PET Procedures*

[$^{11}$C]yohimbine was synthesized as previously described [29]. The radiochemical purities of syntheses used for the study were greater than 95%, with corresponding molar activities of 70 ± 29 GBq/μmol at the end of synthesis. All subjects received an intravenous bolus injection of 370 MBq ± 10% of [$^{11}$C]yohimbine. List-mode PET data were acquired, during the 90 min from the injection of the tracer, simultaneously with 3T MRI data (Dixon T1, anatomic MPRAGE T1) on a Siemens mMR Biograph system.

### *2.3. Image Processing*

Raw PET data were motion corrected [30], and then rebinned into 24 time frame (variable length frames, 8 × 15 s, 3 × 60 s, 5 × 120 s, 1 × 300 s, 7 × 600 s) sinograms for dynamic reconstruction. Images were reconstructed using 3D ordinary Poisson-ordered subset expectation maximization (OP-OSEM 3D), incorporating the system point spread function using 3 iterations of 21 subsets. Sinograms were corrected for scatter, randoms, normalization, and attenuation [31]. Reconstructions were performed with a zoom of 2 in a matrix of 172 × 172 voxels, yielding a voxel size of 2.03 × 2.03 × 2.08 mm$^3$, with a 4 mm 3D post-reconstruction Gaussian filtering. Individual MRI T1 was normalized to the MNI space (Montreal Neurological Institute template of the International Consortium for Brain Mapping Project) using the Segment function of SPM 12 [32]. Labeling of the structural brain regions was performed using the multi-atlas propagation with enhanced registration (MAPER) methodology [33], and the 83-region Hammers atlas [34]. After segmentation, regional time–activity curves (TAC) were extracted, and the non-displaceable binding potential ($BP_{ND}$) obtained with the Simplified Reference Tissue Model (SRTM) was calculated in the different ROIs with the corpus callosum taken as the reference region [28].

### *2.4. Statistical Analysis*

Statistical analysis was performed using Rstudio (https://github.com/rstudio/rstudio, accessed on 1 September 2022). Results with $p < 0.05$ were considered statistically significant. First, we conducted a coarse-grained analysis by applying a 13 ROI (Hippocampus,

Occipital Lobe, Cingulate Gyrus, Frontal Lobe, Parietal Lobe, Thalamus, Parahippocampus, Insula, Temporal Lobe, Basal Ganglia, Amygdala, Cerebellum, Raphe nucleus) × 2 side (left, right) × 2 sex (male, female) ANOVA. Then, we performed fine-grained analyses by fractionating the 6 main ROIs according to the Hammers atlas [34]. For each one of these main ROIs (Occipital lobe, Cingulate gyrus, Frontal Lobe, Parietal Lobe, Temporal Lobe, Basal Ganglia), a *n* Subregion (varying from 2 to 9 according to the ROI) × 2 side (left, right) × 2 gender (male, female) ANOVA was performed.

For illustrative purposes only, SPM12 was used for whole brain voxel-based analysis on the spatially normalized and smoothed parametric BP images of the 46 control subjects. To assess sex-related variability, we applied a two-sample *t* test between males and females, with individual BP values taken as covariates for interindividual adjustment. Statistical parametric maps of the *t* statistic were computed with a threshold of $p = 0.005$ uncorrected at the voxel level.

## 3. Results

### *3.1. Regional ROI Analysis*

Table 1 shows $BP_{ND}$ values for the 13 anatomical regions. The results show a main effect of region ($F(11, 4090) = 118.53$, $p < 0.001$) (Table 2) as well as a main effect of sex ($F(1, 4090) = 29.11$, $p < 0.001$) without significant difference between sides ($p = 0.1$). An interaction between sex and region ($F(11, 4090) = 2.63$, $p < 0.005$) indicates that significant differences between females and males are observed in the cerebellum ($p = 0.01$), the frontal and parietal lobes ($p < 0.001$), and the hippocampus ($p < 0.001$). As there was no significant difference between left and right $BP_{ND}$, values were pooled to determine the mean $BP_{ND}$ and the standard deviation (SD) within each ROI (Table 1).

**Table 1.** Regional distribution of $\alpha_2$-ARs in the human brain.

| | [$^{11}$C]yohimbine $BP_{ND}$ | | |
|---|---|---|---|
| | **Females** | **Males** | **All** |
| Hippocampus | **0.67 ± 0.23** | **0.55 ± 0.17** | 0.61 ± 0.21 |
| Occipital Lobe | 0.57 ± 0.21 | 0.60 ± 0.20 | 0.58 ± 0.20 |
| Cingulate Gyrus | 0.55 ± 0.14 | 0.56 ± 0.15 | 0.56 ± 0.14 |
| Frontal Lobe | **0.50 ± 0.17** | **0.54 ± 0.16** | 0.52 ± 0.17 |
| Parietal Lobe | **0.45 ± 0.13** | **0.51 ± 0.14** | 0.48 ± 0.14 |
| Thalamus | 0.46 ± 0.16 | 0.49 ± 0.13 | 0.48 ± 0.15 |
| Parahippocampus | 0.42 ± 0.12 | 0.44 ± 0.12 | 0.43 ± 0.12 |
| Insula | 0.42 ± 0.13 | 0.43 ± 0.15 | 0.42 ± 0.14 |
| Temporal Lobe | 0.36 ± 0.14 | 0.39 ± 0.15 | 0.38 ± 0.14 |
| Basal Ganglia | 0.30 ± 0.18 | 0.32 ± 0.18 | 0.31 ± 0.18 |
| Amygdala | 0.29 ± 0.10 | 0.30 ± 0.10 | 0.30 ± 0.10 |
| Cerebellum | **0.23 ± 0.18** | **0.31 ± 0.12** | 0.27 ± 0.16 |
| Raphe | 0.22 ± 0.16 | 0.26 ± 0.18 | 0.24 ± 0.17 |

Bold values indicate an effect of sex.

**Table 2.** Statistical differences in [$^{11}$C]yohimbine binding between regions.

| | Hippocampus | Occipital Lobe | Cingulate Gyrus | Frontal Lobe | Parietal Lobe | Thalamus | Parahippocampus | Insula | Temporal Lobe | Basal Ganglia | Amygdala | Cerebellum | Raphe |
|---|---|---|---|---|---|---|---|---|---|---|---|---|---|
| Hippocampus | | | | | | | | | | | | | |
| Occipital Lobe | ns | | | | | | | | | | | | |
| Cingulate Gyrus | ns | ns | | | | | | | | | | | |
| Frontal Lobe | *** | *** | ns | | | | | | | | | | |
| Parietal Lobe | *** | *** | *** | *** | | | | | | | | | |
| Thalamus | *** | *** | * | ns | ns | | | | | | | | |
| Parahippocampus | *** | *** | *** | *** | ns | ns | | | | | | | |
| Insula | *** | *** | *** | *** | *** | ns | ns | | | | | | |
| Temporal Lobe | *** | *** | *** | *** | *** | *** | ns | *** | | | | | |
| Basal Ganglia | *** | *** | *** | *** | *** | *** | *** | *** | *** | | | | |
| Amygdala | *** | *** | *** | *** | *** | *** | *** | *** | ** | ns | | | |
| Cerebellum | *** | *** | *** | *** | *** | *** | *** | *** | *** | ns | ns | | |
| Raphe | *** | *** | *** | *** | *** | *** | *** | *** | *** | ** | ns | ns | |

ns: nonsignificant (ps > 0.1), *** = $p < 0.0005$, ** = $p < 0.005$, * = $p < 0.05$.

### *3.2. Subregional ROI Analyses*

Within the occipital lobe, a significant main effect of region is observed ($F(2, 264) = 87.5$; $p < 0.001$) showing that [$^{11}$C]yohimbine $BP_{ND}$ is not different between the cuneus ($0.69 \pm 0.17$) and the lingual gyrus ($0.66 \pm 0.17$), two regions characterized by a stronger BP than the lateral parts of the occipital lobe ($0.40 \pm 0.14$, ps < 0.001).

Within the cingulate gyrus, a significant main effect of region is reported ($F(1, 176) = 24.6$; $p < 0.001$), showing that [$^{11}$C]yohimbine $BP_{ND}$ is higher in its posterior part (PCC, $0.61 \pm 0.14$) than in its anterior part (ACC, $0.51 \pm 0.13$).

Within the frontal lobe, significant main effects of sex and regions are observed, without interaction. Males have overall higher [$^{11}$C]yohimbine $BP_{ND}$ than females ($F(1, 1068) = 16.7$ $p < 0.001$). Among the frontal subregions, the highest [$^{11}$C]yohimbine $BP_{ND}$ is found within the straight gyrus ($0.65 \pm 0.15$), followed by the orbital gyrus ($0.58 \pm 0.16$), the presubgenual ACC ($0.57 \pm 0.16$), and the middle frontal gyrus ($0.54 \pm 0.15$). Intermediate [$^{11}$C]yohimbine $BP_{ND}$ is observed in the superior frontal gyrus ($0.51 \pm 0.15$), the inferior frontal gyrus ($0.49 \pm 0.13$), the precentral gyrus ($0.43 \pm 0.14$), and the subgenual ACC ($0.42 \pm 0.13$), while the lowest [$^{11}$C]yohimbine $BP_{ND}$ is observed in the subcallosal area ($0.36 \pm 0.13$). *p*-value thresholds are shown in Table 3.

Within the parietal lobe, only a significant effect of sex is observed ($F(1, 352) = 14.16$; $p < 0.001$), with males ($0.51 \pm 0.14$) having overall higher [$^{11}$C]yohimbine $BP_{ND}$ than females ($0.45 \pm 0.13$).

Within the temporal lobe, significant main effects of sex ($F(1, 624) = 4.2$; $p = 0.04$), side ($F(1, 624) = 15.03$; $p < 0.001$), and region ($F(4, 624) = 22.2$; $p < 0.001$) are observed with no significant interaction between the three independent variables. Males ($0.39 \pm 0.15$) have overall higher [$^{11}$C]yohimbine $BP_{ND}$ than females ($0.36 \pm 0.14$). $BP_{ND}$ is higher on the right side ($0.40 \pm 0.14$) than on the left side ($0.36 \pm 0.14$). Finally, [$^{11}$C]yohimbine $BP_{ND}$ is higher in the posterior temporal lobe ($0.47 \pm 0.13$) than in a group of subregions composed of the fusiform gyrus ($0.41 \pm 0.13$), the superior temporal gyrus ($0.38 \pm 0.15$), and in the middle and inferior temporal gyrus ($0.37 \pm 0.12$) which show intermediate binding levels. A lower [$^{11}$C]yohimbine $BP_{ND}$ was reported in the anterior temporal lobe ($0.32 \pm 0.13$).

Within the basal ganglia, a significant main effect of region is reported ($F(4, 440) = 60.54$; $p < 0.001$) showing that [$^{11}$C]yohimbine $BP_{ND}$ is higher in the nucleus accumbens ($0.41 \pm 0.14$), the putamen ($0.40 \pm 0.17$), and the pallidum ($0.39 \pm 0.15$) than in the substantia nigra ($0.19 \pm 0.14$) and the caudate ($0.17 \pm 0.12$).

We summarized all the $BP_{ND}$ values in Table 4.

**Table 3.** Differences in [$^{11}$C]yohimbine binding between subregions of the frontal lobe.

| | **Inferior Frontal Gyrus** | **Middle Frontal Gyrus** | **Orbital Gyrus** | **Precentral Gyrus** | **Presubgenual ACC** | **Straight Gyrus** | **Subcallosal Area** | **Subgenual ACC** | **Superior Frontal Gyrus** |
|---|---|---|---|---|---|---|---|---|---|
| Inferior Frontal Gyrus | | | | | | | | | |
| Middle Frontal Gyrus | ns | | | | | | | | |
| Orbital Gyrus | **** | ns | | | | | | | |
| Precentral Gyrus | ns | **** | **** | | | | | | |
| Presubgenual ACC | * | ns | ns | **** | | | | | |
| Straight Gyrus | **** | **** | *** | **** | ** | | | | |
| Subcallosal Area | **** | **** | **** | * | **** | **** | | | |
| Subgenual ACC | ns | **** | **** | ns | **** | **** | ns | | |
| Superior Frontal Gyrus | ns | ns | ** | * | ns | **** | **** | *** | |

(ns: nonsignificant, **** = $p < 0.001$, *** = $p < 0.005$, ** = $p < 0.01$, * = $p < 0.05$).

**Table 4.** Subregional distribution of $\alpha_2$-ARs in the human brain in fractionated ROIs. Bold values indicate an effect of sex.

| | **[$^{11}$C]yohimbine $BP_{ND}$** | | |
|---|---|---|---|
| | **Females** | **Males** | **All** |
| Cuneus | 0.67 ± 0.17 | 0.71 ± 0.16 | 0.68 ± 0.17 |
| Lingual Gyrus | 0.65 ± 0.18 | 0.67 ± 0.16 | 0.66 ± 0.17 |
| Straight Gyrus | 0.65 ± 0.15 | 0.65 ± 0.14 | 0.65 ± 0.14 |
| Posterior Cingulate Cortex | 0.60 ± 0.15 | 0.62 ± 0.14 | 0.61 ± 0.14 |
| Hippocampus | **0.67 ± 0.23** | **0.55 ± 0.17** | 0.61 ± 0.21 |
| Orbital Gyrus | **0.55 ± 0.17** | **0.60 ± 0.14** | 0.58 ± 0.16 |
| Presubgenual ACC | 0.56 ± 0.18 | 0.57 ± 0.15 | 0.57 ± 0.16 |
| Middle Frontal Gyrus | **0.49 ± 0.14** | **0.58 ± 0.16** | 0.54 ± 0.15 |
| Anterior Cingulate Cortex | 0.51 ± 0.12 | 0.51 ± 0.14 | 0.51 ± 0.13 |
| Superior Frontal Gyrus | **0.49 ± 0.15** | **0.53 ± 0.15** | 0.51 ± 0.15 |
| Superior Parietal Gyrus | **0.47 ± 0.13** | **0.52 ± 0.14** | 0.50 ± 0.14 |
| Inferior Frontal Gyrus | **0.46 ± 0.11** | **0.51 ± 0.14** | 0.49 ± 0.13 |
| Supramarginal Gyrus | **0.46 ± 0.13** | **0.50 ± 0.14** | 0.48 ± 0.14 |
| Angular Gyrus | **0.44 ± 0.14** | **0.51 ± 0.15** | 0.48 ± 0.15 |
| Thalamus | 0.46 ± 0.16 | 0.49 ± 0.13 | 0.48 ± 0.15 |
| Posterior Temporal Lobe | **0.46 ± 0.13** | **0.48 ± 0.13** | 0.47 ± 0.13 |
| Postcentral Gyrus | **0.43 ± 0.13** | **0.49 ± 0.14** | 0.46 ± 0.14 |
| Parahippocampus | 0.42 ± 0.12 | 0.44 ± 0.12 | 0.43 ± 0.12 |
| Precentral Gyrus | **0.40 ± 0.13** | **0.46 ± 0.14** | 0.43 ± 0.14 |
| Subgenual ACC | 0.42 ± 0.13 | 0.41 ± 0.12 | 0.42 ± 0.13 |
| Insula | 0.42 ± 0.13 | 0.43 ± 0.15 | 0.42 ± 0.14 |
| Fusiform gyrus | 0.41 ± 0.12 | 0.41 ± 014 | 0.41 ± 0.13 |
| Nucleus Accumbens | 0.40 ± 0.16 | 0.41 ± 0.13 | 0.41 ± 0.14 |
| Lateral Occipital Lobe | 0.39 ± 0.13 | 0.42 ± 0.14 | 0.40 ± 0.14 |
| Putamen | 0.37 ± 0.18 | 0.43 ± 0.17 | 0.40 ± 0.17 |
| Pallidum | 0.37 ± 0.14 | 0.41 ± 0.16 | 0.39 ± 0.15 |
| Superior Temporal Gyrus | **0.36 ± 0.14** | **0.39 ± 0.16** | 0.38 ± 0.15 |
| Middle and Inferior Temporal Gyrus | 0.37 ± 0.12 | 0.36 ± 0.13 | 0.37 ± 0.12 |

**Table 4.** *Cont.*

| | [$^{11}$C]yohimbine $BP_{ND}$ | | |
|---|---|---|---|
| | **Females** | **Males** | **All** |
| Subcallosal Area | 0.36 ± 0.14 | 0.35 ± 0.12 | 0.35 ± 0.13 |
| Anterior Temporal Lobe | **0.30 ± 0.13** | **0.33 ± 0.13** | 0.32 ± 0.13 |
| Amygdala | 0.29 ± 0.10 | 0.30 ± 0.10 | 0.30 ± 0.10 |
| Cerebellum | **0.23 ± 0.18** | **0.31 ± 0.12** | 0.27 ± 0.16 |
| Raphe | 0.22 ± 0.16 | 0.26 ± 0.18 | 0.24 ± 0.17 |
| Substantia Nigra | 0.20 ± 0.14 | 0.19 ± 0.14 | 0.19 ± 0.14 |
| Caudate Nucleus | 0.15 ± 0.14 | 0.19 ± 0.09 | 0.17 ± 0.12 |

### *3.3. Whole Brain Illustrations*

The distribution of $\alpha_2$-ARs in the living human brain can be illustrated using the average parametric images of [$^{11}$C]yohimbine $BP_{ND}$ values overlaid on an average T1-weighted image of the 46 subjects (Figure 1).

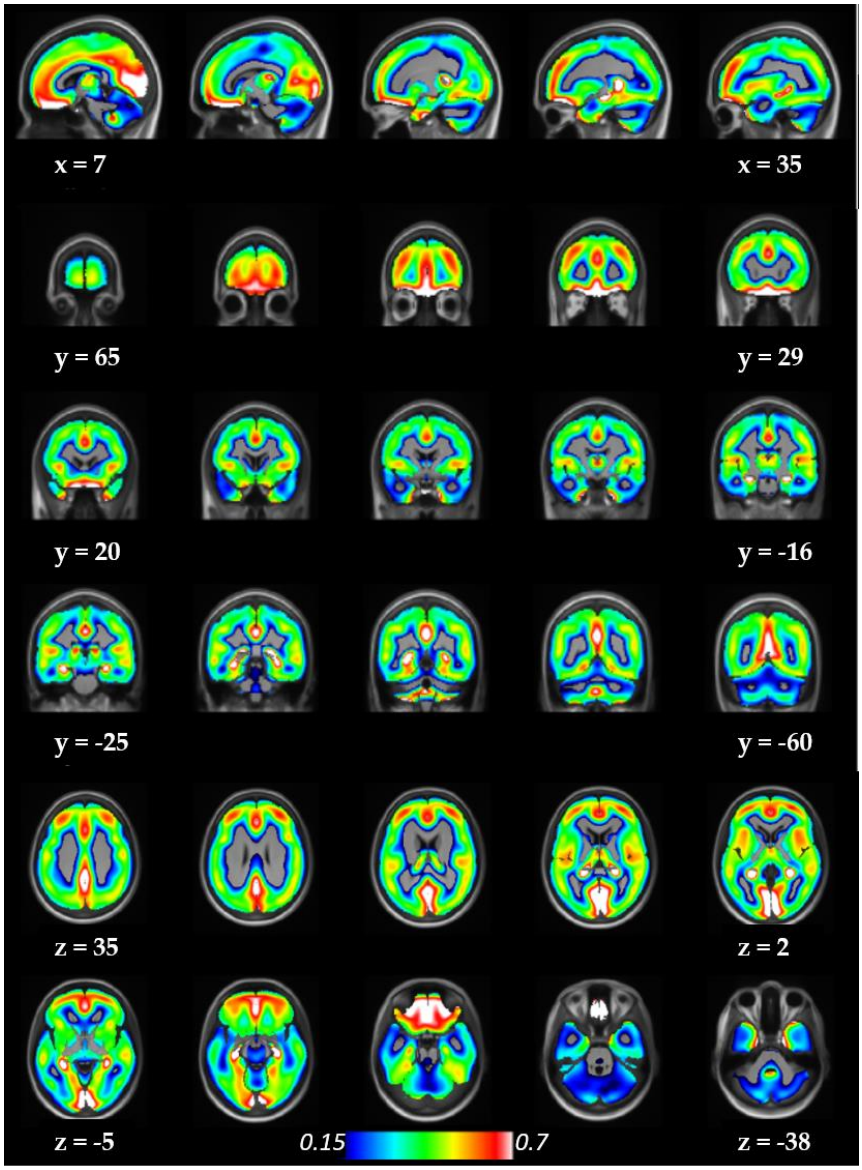


**Figure 1.** Widespread distribution of $\alpha_2$-ARs in the living human brain. Color bar gives estimates of $BP_{ND}$ in units of $mL.cm^{-3}$. In order to facilitate the use of this map, the average parametric image of

$BP_{ND}$ values of this dataset can be downloaded and used for any purpose with a simple request to the corresponding author.

The gender effect found in the main coarse-grained and fine-grained statistical analyses can be illustrated using the statistical parametric maps comparing females to males (Figure 2).

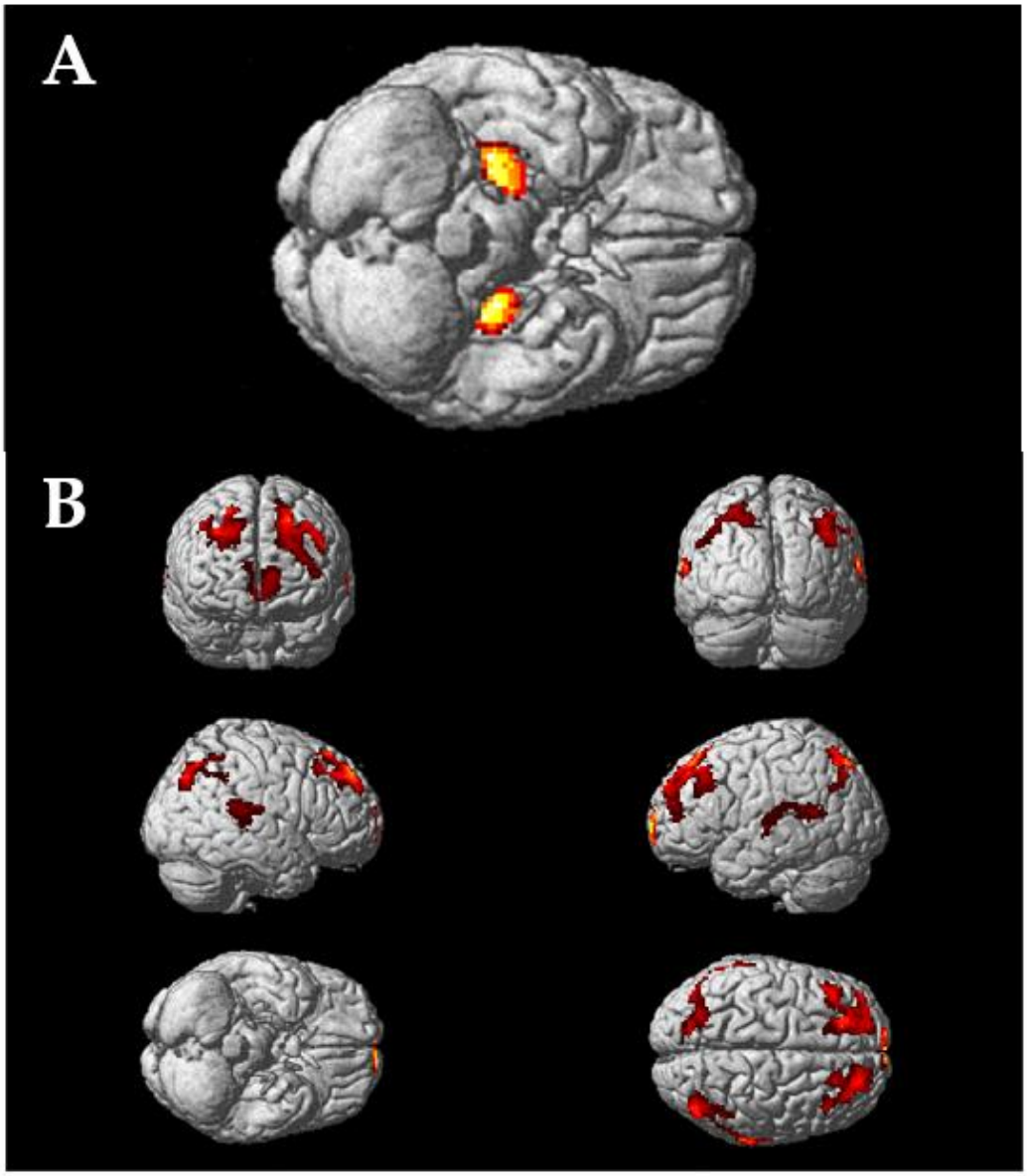


**Figure 2.** Statistical parametric maps comparing females to males. Data are surface-rendered onto the T1-weighted average reference brain provided by SPM12 using a voxel threshold of $p < 0.005$ (uncorrected) without cluster correction (k = 100 voxels). (**A**) Increase in [$^{11}$C]yohimbine binding in female compared with male subjects is observed bilaterally in the hippocampus. (**B**) Increase in [$^{11}$C]yohimbine binding in male compared with female subjects is observed in the orbital gyrus, superior frontal gyrus, and the middle and superior temporal gyrus, as well as the superior parietal and angular gyrus.

## 4. Discussion

In this paper, we present for the first time a complete human brain mapping of the $\alpha_2$-ARs in vivo. Our data confirm the widespread distribution of these receptors throughout the human brain. The regional distribution of [$^{11}$C]yohimbine binding is broadly consistent with the major findings of post-mortem human brain studies [17,19–22], further validating

the use of the radiotracer. More specifically, the present dataset provides a complete and refined picture of subregional variations in $\alpha_2$-ARs based on 35 anatomical subdivisions of the Hammers' probabilistic atlas [34,35]. This statistical mapping is intended to provide a tool for interpreting current issues on the physiological bases of NA functions in the human brain and for conducting future investigations of the role of $\alpha_2$-ARs in regulating NA neurotransmission in healthy and clinical conditions. Furthermore, this statistical mapping also raises new issues such as gender effects.

### *4.1. Regional Distribution of [$^{11}$C]yohimbine*

Important regional variations of $\alpha_2$-ARs availability are observed. The highest [$^{11}$C]yohimbine binding was seen in the hippocampus followed by the occipital lobe, the cingulate gyrus, and the frontal lobe. Regions with moderate levels of specific binding included the parietal lobe, the thalamus, the parahippocampus, the insula, and the temporal lobe. Low [$^{11}$C]yohimbine binding was found in the basal ganglia, amygdala, cerebellum, and raphe nucleus. This broad overview does not contradict quantitative autoradiographic studies [16,18,20,21,24].

### *4.2. Subregional Variations in $\alpha_2$-ARs Availability*

With the exception of the parietal lobe showing remarkable homogeneity (with intermediate to high levels of binding), parcellating the brain into anatomical subregions pinpoints important variations of [$^{11}$C]yohimbine binding within each structure.

The occipital lobe presents a substantial variation of specific binding ranging from very high to intermediate/low, with the medial structures of the visual cortex (cuneus and lingual gyrus) showing the highest binding of all ROIs, whereas the lateral parts of the occipital lobe are characterized by a binding level comparable to structures of the basal ganglia. This strong heterogeneity has been ignored in previous studies, either because only medial regions were examined (e.g., primary visual cortex) [20,21,23] or because global indexes of occipital binding were calculated [24].

The frontal lobe is also characterized by high heterogeneity (Table 3 and Figure 2). A high level of binding was found in the presubgenual ACC and in the straight, orbital, and middle frontal gyri. A medium level of binding was found in the subgenual ACC and in the inferior, superior, and prefrontal gyri. A low level of binding was found in the subcallosal area. These variations were not detected, or even taken in account, in previous autoradiographic studies of the frontal cortex with only a few numbers of subregions of interest (e.g., BA 9 in [17,36,37]; BA 8–9 in [38]; BA 10 in [22]). This observation may prove crucial for understanding the complex and controversial roles of the NA system in the many functions supported by the frontal lobe [39–43].

Interestingly, while the basal ganglia as a whole shows [$^{11}$C]yohimbine binding lying in the low range (Table 1), it is worth mentioning that there are important regional variations between the different nuclei. While the nucleus accumbens, the putamen and pallidum show intermediate binding, and the caudate and the substantia nigra exhibit almost negligible binding (Table 4). This complements the former observation obtained with experimental animal studies, which revealed higher levels of the $\alpha_{2A}$-ARs in the nucleus accumbens than in the caudate [44].

Finally, subregions of the thalamus could not be assessed with the Hammers atlas. However, in contrast to the above data, heterogeneous distribution of $\alpha_2$-ARs is expected from human [21] and animal literature [45,46], with concentrations in the midline, pulvinar, and posterior (intralaminar) nuclei as well as in visual and auditory relay nuclei (geniculate nuclei).

### *4.3. New Issues*

Our consistent sample of subjects allowed for statistical comparisons between women and men. For the first, differences were found in the hippocampus, cerebellum, and frontal and parietal lobes. Interestingly, while the [$^{11}$C]yohimbine binding in the hippocampus was higher for females than males, the opposite pattern was observed in the other regions.

The higher $BP_{ND}$ could reflect changes in both pre- and postsynaptic receptors. On the one hand, it can be interpreted as reflecting a higher density of $\alpha_2$-ARs, but on the other hand, higher $BP_{ND}$ values can also be interpreted as reflecting a higher availability of $\alpha_2$-ARs sites due to a lower concentration of NA (given that [$^{11}$C]yohimbine is sensitive to endogenous variations of NA concentration [47]). This effect could be explained by the fact that central $\alpha_2$-ARs function would be attenuated by estrogen concentration and, as a consequence, would be relatively "blunted" in females. Some arguments come from animal studies showing that hypothalamic $\alpha_2$-ARs decrease following estrogen treatment in ovariectomized rats [48,49], leading $\alpha_2$-AR-mediated inhibition of NA release [50,51]. Further arguments come from clinical studies showing a gender effect in the prevalence of $\alpha_2$-AR-related disorders, such as mood and anxiety [52], which are almost twice as high in females than in males [53]. Our results highlight the need to consider this gender effect in all types of studies of the NA system.

### *4.4. Limitations*

The main limitation of the present study, and by extension of the use of [$^{11}$C]yohimbine PET, is the fact that it does not differentiate between the different subtypes of $\alpha_2$-ARs that have been characterized pharmacologically ($\alpha_{2A}$, $\alpha_{2B}$, $\alpha_{2C}$) [54]. The physiological relevance of these subtypes cannot be fully elucidated without specific radioligands, but the differences that have already been identified between the different $\alpha_2$ receptor subtypes must be acknowledged for interpreting [$^{11}$C]yohimbine PET data. In particular, the $\alpha_{2A}$-subytpe is known to be the main inhibitory presynaptic feedback receptor [55–57] with $\alpha_{2C}$ to a less extent. These two subtypes are also known as heteroceptors that inhibit the release of dopamine and serotonin [58,59] making the problem even more complex. In addition, there are $\alpha_2$-ARs both at the pre- and postsynaptic sites, which always makes interpretation of the results difficult. Nevertheless, it is broadly considered that the presynaptic inhibitory autoreceptors located on noradrenergic neurons in the locus coeruleus play a crucial role in the regulation of the release and synthesis of noradrenaline, while the postsynaptic $\alpha_2$-ARs located in the widely distributed projection areas of the neurons throughout the cortex modulate the signaling pathways [60,61]. Finally, it must be acknowledged that we did not apply partial volume correction, meaning that these data must be interpreted with caution, in particular with regard to the relative low binding in small structures or to the absence of differences between nearby regions due to the spillover effect.

## 5. Conclusions

The $\alpha_2$-ARs play a key role in regulating NA neurotransmission [62,63], but their in vivo imaging in humans was not possible until now. Providing a technical solution, [$^{11}$C]yohimbine PET allowed for the mapping of their distribution in the living human brain, which will help interpreting past and future investigations on the role of the NA system in numerous brain functions in healthy as well as in various clinical conditions. This is all the more important as altered NA transmission with specific loss of $\alpha_2$-ARs is currently suspected to play a critical role in both the symptoms and progression of some neurodegenerative and mood disorders [9,22].

**Author Contributions:** Conceptualization, C.L., S.L., P.B. and B.B.; methodology, S.L., N.C. and B.B.; software, I.M., J.R. and N.C.; validation, S.L. and D.L.B.; formal analysis, C.L., I.M., N.C. and B.B.; investigation, C.L., S.L., I.M., N.C., D.L.B. and B.B.; resources, P.B. and B.B.; data curation, B.B.; writing—original draft preparation, P.B. and B.B.; writing—review and editing, C.L., S.L., I.M., N.C., J.R., P.B. and B.B.; visualization, C.L., P.B. and B.B.; supervision, B.B.; project administration, B.B.; funding acquisition, B.B. All authors have read and agreed to the published version of the manuscript.

**Funding:** This research was funded by the French National Agency of Research (grant number ANR-16-CE37-0014 to B.B).

**Institutional Review Board Statement:** The study was conducted in accordance with the Declaration of Helsinki and approved by the local Ethical Committee in Biomedical Research (N° CPP 19_01_02/N°EudraCT 2018-003999-13).

**Informed Consent Statement:** Informed consent was obtained from all subjects involved in the study.

**Data Availability Statement:** The authors will be happy to support request for a formal data sharing agreement.

**Conflicts of Interest:** The authors declare no conflict of interest. The funders had no role in the design of the study; in the collection, analyses, or interpretation of data; in the writing of the manuscript; or in the decision to publish the results.

## References


1. Holland, N.; Robbins, T.W.; Rowe, J.B. The Role of Noradrenaline in Cognition and Cognitive Disorders. *Brain* **2021**, *144*, 2243–2256. [CrossRef] [PubMed]
2. Sara, S.J.; Bouret, S. Orienting and Reorienting: The Locus Coeruleus Mediates Cognition through Arousal. *Neuron* **2012**, *76*, 130–141. [CrossRef] [PubMed]
3. Berridge, C.W.; Waterhouse, B.D. The Locus Coeruleus–Noradrenergic System: Modulation of Behavioral State and State-Dependent Cognitive Processes. *Brain Res. Rev.* **2003**, *42*, 33–84. [CrossRef] [PubMed]
4. Aston-Jones, G.; Cohen, J.D. Adaptive Gain and the Role of the Locus Coeruleus-Norepinephrine System in Optimal Performance. *J. Comp. Neurol.* **2005**, *493*, 99–110. [CrossRef] [PubMed]
5. Singh, S. Noradrenergic Pathways of Locus Coeruleus in Parkinson's and Alzheimer's Pathology. *Int. J. Neurosci.* **2020**, *130*, 251–261. [CrossRef]
6. Weinshenker, D. Long Road to Ruin: Noradrenergic Dysfunction in Neurodegenerative Disease. *Trends Neurosci.* **2018**, *41*, 211–223. [CrossRef]
7. Shin, E.; Rogers, J.T.; Devoto, P.; Björklund, A.; Carta, M. Noradrenaline Neuron Degeneration Contributes to Motor Impairments and Development of L-DOPA-Induced Dyskinesia in a Rat Model of Parkinson's Disease. *Exp. Neurol.* **2014**, *257*, 25–38. [CrossRef]
8. Delaville, C.; Deurwaerdère, P.D.; Benazzouz, A. Noradrenaline and Parkinson's Disease. *Front. Syst. Neurosci.* **2011**, *5*, 31. [CrossRef]
9. Marien, M.R.; Colpaert, F.C.; Rosenquist, A.C. Noradrenergic Mechanisms in Neurodegenerative Diseases: A Theory. *Brain Res. Rev.* **2004**, *45*, 38–78. [CrossRef]
10. Braak, H.; Tredici, K.D.; Rüb, U.; de Vos, R.A.I.; Jansen Steur, E.N.H.; Braak, E. Staging of Brain Pathology Related to Sporadic Parkinson's Disease. *Neurobiol. Aging* **2003**, *24*, 197–211. [CrossRef]
11. Cui, K.; Yang, F.; Tufan, T.; Raza, M.U.; Zhan, Y.; Fan, Y.; Zeng, F.; Brown, R.W.; Price, J.B.; Jones, T.C.; et al. Restoration of Noradrenergic Function in Parkinson's Disease Model Mice. *ASN Neuro* **2021**, *13*, 175909142110097. [CrossRef] [PubMed]
12. Caraci, F.; Merlo, S.; Drago, F.; Caruso, G.; Parenti, C.; Sortino, M.A. Rescue of Noradrenergic System as a Novel Pharmacological Strategy in the Treatment of Chronic Pain: Focus on Microglia Activation. *Front. Pharmacol.* **2019**, *10*, 1024. [CrossRef] [PubMed]
13. O'Neill, E.; Harkin, A. Targeting the Noradrenergic System for Anti-Inflammatory and Neuroprotective Effects: Implications for Parkinson's Disease. *Neural Regen. Res.* **2018**, *13*, 1332. [CrossRef] [PubMed]
14. Nutt, D.J.; McAllister–Williams, R.H. Noradrenaline—The Forgotten Amine? *J. Psychopharmacol.* **2013**, *27*, 657–658. [CrossRef]
15. Fornai, F.; di Poggio, A.; Pellegrini, A.; Ruggieri, S.; Paparelli, A. Noradrenaline in Parkinsons Disease: From Disease Progression to Current Therapeutics. *Curr. Med. Chem.* **2007**, *14*, 2330–2334. [CrossRef]
16. Probst, A.; Cortés, R.; Palacios, J.M. Distribution of A2-Adrenergic Receptors in the Human Brainstem: An Autoradiographic Study Using [3H]p-Aminoclonidine. *Eur. J. Pharmacol.* **1984**, *106*, 477–488. [CrossRef]
17. Pazos, A. Aa-Adrenoceptors in Human Forebrain: Autoradiographic Visualization and Biochemical Parameters Using the Agonist [AH]UK-14304. *Brain Res.* **1988**, *475*, 361–365. [CrossRef]
18. Jones, C.R.; Palacios, J.M. Autoradiography of Adrenoceptors in Rat and Human Brain: α-Adrenoceptor and Idazoxan Binding Sites. In *Progress in Brain Research*; Elsevier: Amsterdam, The Netherlands, 1991; Volume 88, pp. 271–291. ISBN 978-0-444-81394-7.
19. Vos, H.; Vauquelin, G.; Keyser, J.; Backer, J.-P.; Liefde, I. Regional Distribution of $\alpha_{2A}$- and $\alpha_{2B}$-Adrenoceptor Subtypes in Postmortem Human Brain. *J. Neurochem.* **1992**, *58*, 1555–1560. [CrossRef]
20. Pascual, J.; Del Arco, C.; Gonzalez, A.; Diaz, A.; del Olmo, E.; Pazos, A. Regionally Specific Age-Dependent Decline in α2-Adrenoceptors: An Autoradiograpic Study in Human Brain. *Neurosci. Lett.* **1991**, *133*, 279–283. [CrossRef]
21. Pascual, J.; del Arco, C.; Gonzalez, A.; Pazos, A. Quantitative Light Microscopic Autoradiographic Localization of A2-Adrenoceptors in the Human Brain. *Brain Res.* **1992**, *582*, 116–127. [CrossRef]
22. Ordway, G.A.; Jaconetta, S.M.; Halaris, A.E. Characterization of Subtypes of Alpha-2 Adrenoceptors in the Human Brain. *J. Pharmacol. Exp. Ther.* **1993**, *264*, 967–976. [PubMed]
23. Fagerholm, V.; Rokka, J.; Nyman, L.; Sallinen, J.; Tiihonen, J.; Tupala, E.; Haaparanta, M.; Hietala, J. Autoradiographic Characterization of A2C-Adrenoceptors in the Human Striatum. *Synapse* **2008**, *62*, 508–515. [CrossRef] [PubMed]

24. Vos, H.D.; Convents, A.; Keyser, J.D.; Backer, J.-P.D.; Megena, V.; Ebinger, G.; Vauquelin, G. Autoradiographic Distribution of A2 Adrenoceptors, NAIBS, and 5-I-IT1A Receptors in Human Brain Using [3H]Idazoxan and [3H]Rauwolscine. *Brain Res.* **1991**, *566*, 13–20. [CrossRef] [PubMed]
25. Sastre, M.; Garcia-Sevilla, J.A. Opposite Age-Dependent Changes of A2A-Adrenoceptors and Nonadrenoceptor [3H]Idazoxan Binding Sites (I2-Imidazoline Sites) in the Human Brain: Strong Correlation of I2 with Monoamine Oxidase-B Sites. *J. Neurochem.* **1993**, *61*, 881–889. [CrossRef] [PubMed]
26. Biegon, A.; Mathis, C.A.; Budinger, T.F. Quantitative in Vitro and Ex Vivo Autoradiography of the A2-Adrenoceptor Antagonist [3H]Atopamezole. *Eur. J. Pharmacol.* **1992**, *224*, 27–38. [CrossRef]
27. Nahimi, A.; Jakobsen, S.; Munk, O.L.; Vang, K.; Phan, J.A.; Rodell, A.; Gjedde, A. Mapping 2 Adrenoceptors of the Human Brain with 11C-Yohimbine. *J. Nucl. Med.* **2015**, *56*, 392–398. [CrossRef]
28. Laurencin, C.; Lancelot, S.; Gobert, F.; Redouté, J.; Mérida, I.; Iecker, T.; Liger, F.; Irace, Z.; Greusard, E.; Lamberet, L.; et al. Modeling [11C]Yohimbine PET Human Brain Kinetics with Test-Retest Reliability, Competition Sensitivity Studies and Search for a Suitable Reference Region. *NeuroImage* **2021**, *140*, 118328. [CrossRef]
29. Jakobsen, S.; Pedersen, K.; Smith, D.F.; Jensen, S.B.; Munk, O.L.; Cumming, P. Detection of A2-Adrenergic Receptors in Brain of Living Pig with 11C-Yohimbine. *J. Nucl. Med.* **2006**, *47*, 2008–2015.
30. Reilhac, A.; Merida, I.; Irace, Z.; Stephenson, M.C.; Weekes, A.A.; Chen, C.; Totman, J.J.; Townsend, D.W.; Fayad, H.; Costes, N. Development of a Dedicated Rebinner with Rigid Motion Correction for the MMR PET/MR Scanner, and Validation in a Large Cohort of 11C-PIB Scans. *J. Nucl. Med.* **2018**, *59*, 1761–1767. [CrossRef]
31. Mérida, I.; Reilhac, A.; Redouté, J.; Heckemann, R.A.; Costes, N.; Hammers, A. Multi-Atlas Attenuation Correction Supports Full Quantification of Static and Dynamic Brain PET Data in PET-MR. *Phys. Med. Biol.* **2017**, *62*, 2834–2858. [CrossRef]
32. Ashburner, J.; Friston, K.J. Unified Segmentation. *NeuroImage* **2005**, *26*, 839–851. [CrossRef] [PubMed]
33. Heckemann, R.A.; Keihaninejad, S.; Aljabar, P.; Rueckert, D.; Hajnal, J.V.; Hammers, A. Improving Intersubject Image Registration Using Tissue-Class Information Benefits Robustness and Accuracy of Multi-Atlas Based Anatomical Segmentation. *NeuroImage* **2010**, *51*, 221–227. [CrossRef] [PubMed]
34. Hammers, A.; Allom, R.; Koepp, M.J.; Free, S.L.; Myers, R.; Lemieux, L.; Mitchell, T.N.; Brooks, D.J.; Duncan, J.S. Three-Dimensional Maximum Probability Atlas of the Human Brain, with Particular Reference to the Temporal Lobe. *Hum. Brain Mapp.* **2003**, *19*, 224–247. [CrossRef] [PubMed]
35. Heckemann, R.A.; Hajnal, J.V.; Aljabar, P.; Rueckert, D.; Hammers, A. Automatic Anatomical Brain MRI Segmentation Combining Label Propagation and Decision Fusion. *NeuroImage* **2006**, *33*, 115–126. [CrossRef]
36. Javier Meana, J.; Barturen, F.; Asier Garro, M.; García-Sevilla, J.A.; Fontán, A.; Zarranz, J.J. Decreased Density of Presynaptic A2-Adrenoceptors in Postmortem Brains of Patients with Alzheimer's Disease. *J. Neurochem.* **1992**, *58*, 1896–1904. [CrossRef]
37. Meana, J.J.; Barturen, F. α2-Adrenoceptors in the Brain of Suicide Victims: Increased Receptor Density Associated with Major Depression. *Biol. Psychiatry* **1992**, *31*, 471–490. [CrossRef]
38. González, A.M.; Pascual, J.; Meana, J.J.; Barturen, F.; Del Arco, C.; Pazos, A.; García-Sevilla, J.A. Autoradiographic Demonstration of Increased A2-Adrenoceptor Agonist Binding Sites in the Hippocampus and Frontal Cortex of Depressed Suicide Victims. *J. Neurochem.* **1994**, *63*, 256–265. [CrossRef]
39. Yuan, P.; Raz, N. Prefrontal Cortex and Executive Functions in Healthy Adults: A Meta-Analysis of Structural Neuroimaging Studies. *Neurosci. Biobehav. Rev.* **2014**, *42*, 180–192. [CrossRef]
40. Volz, K.G.; Schubotz, R.I.; von Cramon, D.Y. Decision-Making and the Frontal Lobes. *Curr. Opin. Neurol.* **2006**, *19*, 401–406. [CrossRef]
41. Rolls, E.T. The Functions of the Orbitofrontal Cortex. *Brain Cogn.* **2004**, *55*, 11–29. [CrossRef]
42. Schall, J.D.; Stuphorn, V.; Brown, J.W. Monitoring and Control of Action by the Frontal Lobes. *Neuron* **2002**, *36*, 309–322. [CrossRef] [PubMed]
43. Chayer, C.; Freedman, M. Frontal Lobe Functions. *Curr. Neurol. Neurosci. Rep.* **2001**, *1*, 547–552. [CrossRef] [PubMed]
44. Talley, E.M.; Rosin, D.L.; Lee, A.; Guyenet, P.G.; Lynch, K.R. Distribution of α2A-Adrenergic Receptor-like Immunoreactivity in the Rat Central Nervous System. *J. Comp. Neurol.* **1996**, *372*, 111–134. [CrossRef]
45. Strazielle, C.; Lalonde, R.; Hébert, C.; Reader, T.A. Regional Brain Distribution of Noradrenaline Uptake Sites, and of α1-α2- and Beta-Adrenergic Receptors in PCD Mutant Mice: A Quantitative Autoradiographic Study. *Neuroscience* **1999**, *94*, 287–304. [CrossRef] [PubMed]
46. Pérez-Santos, I.; Palomero-Gallagher, N.; Zilles, K.; Cavada, C. Distribution of the Noradrenaline Innervation and Adrenoceptors in the Macaque Monkey Thalamus. *Cereb. Cortex* **2021**, *31*, 4115–4139. [CrossRef]
47. Landau, A.M.; Doudet, D.J.; Jakobsen, S. Amphetamine Challenge Decreases Yohimbine Binding to A2 Adrenoceptors in Landrace Pig Brain. *Psychopharmacology* **2012**, *222*, 155–163. [CrossRef]
48. Wilkinson, M.; Herdon, H.; Pearce, M.; Wilson, C. Radioligand Binding Studies on Hypothalamic Noradrenergic Receptors during the Estrous Cycle or after Steroid Injection in Ovariectomized Rats. *Brain Res.* **1979**, *168*, 652–655. [CrossRef]
49. Wilkinson, M.; Herdon, H.J. Diethylstilbestrol Regulates the Number of A- and -Adrenergic Binding Sites in Incubated Hypothalamus and Amygdala. *Brain Res.* **1982**, *248*, 79–85. [CrossRef]
50. Karkanias, G.B.; Etgen, A.M. Estradiol Reduction of the Agonist High Affinity Form of the Alpha 2-Adrenoceptor in the Hypothalamus of Female Rats: Identification as the Alpha 2D Subtype. *Mol. Pharmacol.* **1994**, *45*, 509–516.

51. Karkanias, G.B.; Etgen, A.M. Estradiol Attenuates Alpha 2-Adrenoceptor-Mediated Inhibition of Hypothalamic Norepinephrine Release. *J. Neurosci.* **1993**, *13*, 3448–3455. [CrossRef]
52. Eaton, W.W.; Kessler, R.C.; Wittchen, H.U.; Magee, W.J. Panic and Panic Disorder in the United States. *Am. J. Psychiatry* **1994**, *151*, 413–420. [CrossRef] [PubMed]
53. Oquendo, M.A.; Ellis, S.P.; Greenwald, S.; Malone, K.M.; Weissman, M.M.; Mann, J.J. Ethnic and Sex Differences in Suicide Rates Relative to Major Depression in the United States. *Am. J. Psychiatry* **2001**, *158*, 1652–1658. [CrossRef] [PubMed]
54. Bylund, D.B. Pharmacological Characteristics of Alpha-2 Adrenergic Receptor Subtypes. *Ann. N. Y. Acad. Sci.* **1995**, *763*, 1–7. [CrossRef] [PubMed]
55. Altman, J.D.; Trendelenburg, A.U.; Macmillan, L.; Bernstein, D.; Limbird, L.; Starke, K.; Kobilka, B.K.; Hein, L. Abnormal Regulation of the Sympathetic Nervous System in α2A-Adrenergic Receptor Knockout Mice. *Mol. Pharmacol.* **1999**, *56*, 154–161. [CrossRef] [PubMed]
56. Hein, L.; Altman, J.D.; Kobilka, B.K. Two Functionally Distinct A2-Adrenergic Receptors Regulate Sympathetic Neurotransmission. *Nature* **1999**, *402*, 181. [CrossRef]
57. Vonend, O.; Habbel, S.; Stegbauer, J.; Roth, J.; Hein, L.; Rump, L.C. α2A-Adrenoceptors Regulate Sympathetic Transmitter Release in Mice Kidneys. *Br. J. Pharmacol.* **2007**, *150*, 121–127. [CrossRef]
58. Bücheler, M.M.; Hadamek, K.; Hein, L. Two A2-Adrenergic Receptor Subtypes, A2A and A2C, Inhibit Transmitter Release in the Brain of Gene-Targeted Mice. *Neuroscience* **2002**, *109*, 819–826. [CrossRef]
59. Scheibner, J.; Trendelenburg, A.U.; Hein, L.; Starke, K. α2-Adrenoceptors Modulating Neuronal Serotonin Release: A Study in α2-Adrenoceptor Subtype-Deficient Mice. *Br. J. Pharmacol.* **2001**, *132*, 925–933. [CrossRef]
60. Langer, S.Z. Presynaptic Regulation of the Release of Catecholamines. *Pharmacol. Rev.* **1980**, *32*, 337–362. [CrossRef]
61. Heal, D.J.; Butler, S.A.; Prow, M.R.; Buckett, W.R. Quantification of Presynaptic α2-Adrenoceptors in Rat Brain after Short-Term DSP-4 Lesioning. *Eur. J. Pharmacol.* **1993**, *249*, 37–41. [CrossRef]
62. Szabadi, E. Functional Neuroanatomy of the Central Noradrenergic System. *J. Psychopharmacol.* **2013**, *27*, 659–693. [CrossRef] [PubMed]
63. Langer, S.Z. Presynaptic Receptors and Modulation of Neurotransmission: Pharmacological Implications and Therapeutic Relevance. *Trends Neurosci.* **1980**, *3*, 110–112. [CrossRef]